Segmental Rotational Diffusion of Spin-Labeled Polystyrene in Dilute Toluene Solution by 9 and 250 GHz ESR

Jan Pilar, Jirí Labský, and Antonín Marek

Institute of Macromolecular Chemistry, Academy of Sciences of the Czech Republic, Prague 162 06, Czech Republic

David E. Budil,† Keith A. Earle, and Jack H. Freed*

Baker Laboratory of Chemistry and Chemical Biology, Cornell University, Ithaca, New York 14853

Received February 7, 2000; Revised Manuscript Received April 4, 2000

ABSTRACT: A copolymer of styrene containing less than 5 mol % of chain units spin-labeled by attachment of the nitroxide via a short tether has been synthesized. ESR spectra of dilute toluene solution of the copolymer have been obtained using 9 and 250 GHz ESR. Parameters characterizing polystyrene segmental rotational diffusion in toluene solution over a broad temperature range have been determined from nonlinear least-squares fits of theoretical ESR spectra to the experimental ESR spectra. The model used was that of relatively fast internal rotation of the nitroxide about its tether, with slower polymer chain segmental motion. Together they lead to effective rotational diffusion with an anisotropic diffusion tensor. In addition, constraints in the form of an orientational potential restrict the range of angles over which this diffusion occurs relative to the polymer backbone, and the latter is assumed to reorient on an ultraslow time scale. This is referred to as a model of microscopic order but macroscopic disorder (MOMD). Rates for the slower polymer chain segmental motion (from the 250 GHz spectra) ranged from 3.6×10^8 s^{-1} at 311 K to 0.15×10^8 s^{-1} at 215 K, with a substantial orientational potential of about $2kT$ over this temperature range. Although there was reasonable agreement between the results obtained at 9 and 250 GHz, there were systematic discrepancies such that the orienting potentials obtained from the 250 GHz spectra were about twice (or more) those from the 9 GHz spectra, and the rotational diffusion tensor components from the 250 GHz spectra were at least twice those from the 9 GHz spectra. This implies a breakdown of the MOMD model for the 9 GHz spectra presumably due to their sensitivity to the slower overall tumbling motion at this low spectral frequency. For the faster "time scale" of the 250 GHz spectra, such a slow motion is "frozen out", rendering these spectra consistent with the MOMD model. Nevertheless, the results at both frequencies yielded a common activation energy, $E_{exp} = 20.7 \pm 1.5$ kJ/mol, which, when corrected for the viscous flow contribution, yielded an $E_a = 11.9 \pm 1.5$ kJ/mol, which is in good agreement with recent results from fluorescence studies.

1. Introduction

Important macroscopic properties shown by different polymers arise from different chemical structures. Understanding these structure−property relationships represents an important subject in polymer research. The study of local segmental dynamics of polymers plays a significant role in understanding these relationships. Dynamics on the length scale of a few monomer units depends strongly on the details of the monomer structure. It is useful to study local chain motions of an isolated chain in dilute solutions before chain−chain interactions are taken into account. In recent years a great deal of effort has been devoted to understanding the local dynamics of polymers utilizing mainly optical[1−3] and NMR[4,5] techniques.

Data characterizing local rotational dynamics of polymer chains in dilute solutions can be obtained by ESR studies of dilute solutions of spin-labeled polymers as well.[6−8] Parameters characterizing rotational diffusion of a nitroxide spin-label may be determined by means of analysis of their ESR spectra in a particular system.[9] Rotational diffusion of a nitroxide spin-label, which is attached to chain segments of the polymer at randomly distributed sites, has frequently been approximated by rotational diffusion of the polymer chain segment to which the spin-label is attached and of an internal rotation of the spin-label about the tether through which it is attached to the polymer chain segment. The contribution of the rotational diffusion of the polymer coil as a whole was neglected for the high molecular mass polymers. The reason for this neglect is based on results found by fluorescence depolarization (e.g., those of Horinaka et al.[10,11]) that the mean relaxation time for rotational reorientation of the anthryl group bound in the middle of the polystyrene main chain had reached its asymptotic value, independent of molecular mass (M_w) for polystyrene with $M_w \approx 10^4$. (We shall critically assess whether this neglect is appropriate for ESR studies.) The polymer chain in dilute solution experiences conformational changes due to trans−gauche transitions of the main chain bonds followed by distortions of neighboring bond lengths and angles as described by a dynamic extension of the rotational isomeric state (DRIS) model.[12] It is frequently assumed that this process effectively yields diffusion of the polymer chain segment that may be approximated as isotropic rotational diffusion, and it may be characterized by rotational diffusion coefficient R_S . Conformational transitions of the bonds of the tether through which the spin-label is attached to the polymer chain are assumed to result in internal rotational diffusion

* Corresponding author: Fax 607-255-0595; e-mail jhf@ccmr.cornell.edu.

†Present address: Department of Chemistry, Northeastern University, 102 Hurtig Hall, Boston, MA 02115.

10.1021/ma0002242 CCC: $19.00
Published on Web 05/23/2000

Chart 1

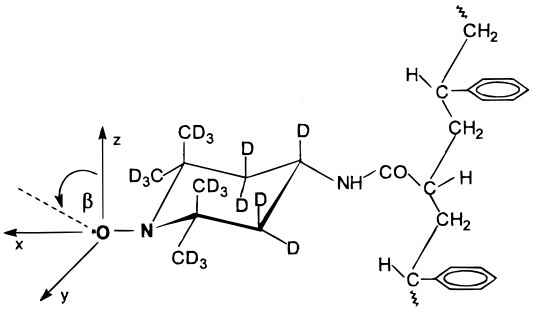

characterized by rotational diffusion coefficient R_I. When the spin-label is attached to the polymer chain via a short tether containing only a single bond about which conformational transitions of the tether can occur, then the axis of internal rotation of the spin-label should be identical to this bond axis.

This approximate model gives rise to axially symmetric rotational diffusion, with two components of the rotational tensor, $R_\perp = R_S$ and $R_\parallel = R_S + R_I, \cong R_I$. In addition, the axis of internal rotation can be tilted relative to the z axis of the nitroxide axis system, and this is specified by angle β. This is shown in Chart 1 for 2,2,6,6-tetramethylpiperidine-*N*-oxyl type spin-labels. This model is known as the VAR (very anisotropic rotation) model, due to Mason et al.[13] In the present case the tether involves three single bonds (C−CO, CO−NH, and NH−SL). Given that the second, which is a peptide bond, is normally fixed, and there are steric constraints on the first, the only bond about which conformational changes of the tether occur is the third bond, NH−SL.

A more successful model for analyzing ESR line shapes from spin-labeled polymers was introduced by Meirovitch et al.[9,14] This model allows for constraints in the above-mentioned motions. More precisely, we regard the polymer chain segmental motion sensed by the tethered nitroxide as restricted by its attachments to the rest of the large M_w polymer. This means that we let the $R_\perp$ motion, i.e., the wobbling motion of the effective internal axis, be constrained by an orienting potential. In addition, there can be asymmetry in the potential resulting from the tether and/or the nitroxide moiety which can affect the $R_\parallel$ motion. Thus, one uses a Smoluchowski equation for the Brownian rotational diffusion, with an orienting potential typically given by

$$-U(\theta,\varphi)/kT = {}^1/_2c_0^2(3\cos^2\theta - 1) + c_2^2[2\sin^2\theta\cos 2\varphi]$$

where the c_0^2 term refers to the restricting potential for the wobbling motion and the c_2^2 to its asymmetry. The angles θ and φ are respectively the polar and azimuthal angles for a unit vector along the preferred orientation for the internal axis in the frame of the polymer with respect to the instantaneous orientation of the tethered nitroxide expressed in the principal axes for its alignment (which for simplicity are assumed to also be the principal axes for its rotational diffusion). This model is known as the MOMD (microscopic order with macroscopic disorder) model.

In the present study our initial analyses showed that the MOMD model led to systematically better fits than the VAR model, so we shall focus in this work on the use and applicability of the MOMD model.

At conventional ESR frequencies (9−35 GHz), rotational dynamics in most fluids is usually sufficiently fast, i.e., $\tau_R\Delta\omega \ll 1$ [where the correlation time $\tau_R = (6)^{-1}(R_\perp{}^2R_\parallel)^{-1/3}$ and $\Delta\omega$ is a measure of the magnitude of the orientation-dependent part of the spin Hamiltonian, which increases with the applied external magnetic field], that such motions fall within the motional narrowing regime.[9] In such cases the ESR spectrum is a simple superposition of Lorentzian lines whose widths cannot be fully and unambiguously related to parameters characterizing the nitroxide rotational diffusion by motional narrowing theory without additional assumptions about the motion. For slower motions, in more viscous media where $\tau_R\Delta\omega \geq 1$, the ESR spectrum depends more dramatically on the combined influences of molecular motion and magnetic interactions. Thus, the slow-motional ESR line shapes, in principle, provide a more detailed picture of rotational dynamics when compared to the motionally narrowed line shapes. These slow-motional line shapes can be fully analyzed by using a theoretical approach based on numerical solution of the stochastic Liouville equation.[9] This has motivated the extension of molecular dynamics studies by ESR to higher magnetic fields requiring resonant radiation at wavelengths on the order of $\lambda \cong 1.2$ mm (250 GHz), corresponding to (FIR) far-infrared ESR.[15−18] Because of the greatly increased $\Delta\omega$ at such frequencies (which require external magnetic fields close to 90 000 G compared with 3300 G required at X-band), rotational motions encountered in liquid phases are more likely to fall into the slow-motional regime, thereby permitting the more detailed analysis.[16,19] Another important feature of such high-frequency studies is the enhanced g-factor resolution, so the regions of the rigid-limit spectrum corresponding to the magnetic x, y, and z components are clearly discerned, and the components of the $\boldsymbol{g}$ tensor may be determined from the rigid-limit spectra with higher accuracy. This increased orientational resolution also has the potential of providing better resolution to the microscopic details of the motions from the slow-motional ESR studies.

Our purpose, in the present work, is to demonstrate the utility of high-frequency ESR experiments together with conventional X-band experiments in studying segmental rotational dynamics of polystyrene in dilute toluene solutions over a broad temperature range.

2. Experimental Section

2.1. Synthesis and Characterization of Spin-Labeled Copolymer. Poly{styrene-*co*-*N*-[2,2,6,6-(tetra[$^2H_3$]methyl)-1-yloxy-(3,3,5,5-[$^2H_4$]-piperidin-4-yl]acrylamide} **(II** in Chart 2). In the first step a mixture of styrene (10 g), acrylic acid (0.5 g), and 2,2′-azobis(2-methylpropionitrile) (0.001 g) was bubbled with argon for 10 min, sealed into an ampule, heated to 60 °C, and copolymerized for 5 h. The ST−AA copolymer **(I)** prepared was dissolved in dioxane and precipitated into methanol. A carboxyl content of 5.3 mol % was found by titration. The mass-average molar mass, M_w equal to 2.6×10^5, was determined by light scattering in dioxane with a modified Sofica 42.000 instrument at 546 nm and 298 K. The refractive index increments were measured under the same conditions with a Brice-Phoenix BP-2000 V differential refractometer. In the second step the ST−AA copolymer **(I)** (2 g) was dissolved in a benzene−dioxane mixture (1:1, 50 mL); after cooling to 5 °C dicyclohexylcarbodiimide (Fluka, 1 g) and 4-amino-2,2,6,6-tetra([$^2H_3$]methyl)(3,3,5,5-[$^2H_4$]-piperidin-1-yloxyl) **(III)** (0.1 g) were added. The reaction mixture was concentrated to approximately 10 mL after standing for 48 h at room temperature, and the spin-labeled copolymer (SL−

Chart 2

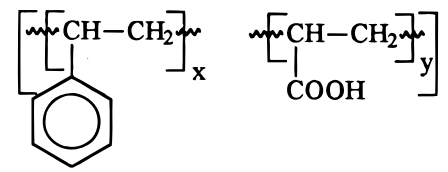

I

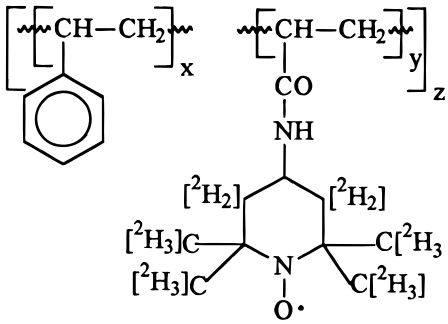

II

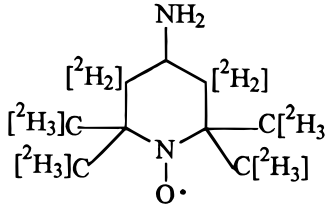

III

ST−AA) **(II)** was precipitated repeatedly into methanol until the ESR spectrum of the free spin-label disappeared completely. The perdeuterated spin-label **(III)** was synthesized locally as described previously.[20]

A dilute solution (1%) of both spin-labeled copolymers in toluene dried over molecular sieves has been prepared for ESR measurements. An equivalent hydrodynamic radius of spin-labeled polymer coils $R_H = 9$ nm was measured by dynamic light scattering (DLS). Polarized DLS measurements were performed at a scattering angle of 90° using a light scattering apparatus equipped with an argon laser (514.5 nm) and an ALV 5000, multibit, multi-tau autocorrelator covering approximately 12 decades in delay time. The correlation functions were analyzed with the program REPES,[21,22] which targets the inverse Laplace transformation. The measurement has simultaneously shown the presence of a negligible concentration of larger aggregates ($R_H \sim 300$ nm).

If not specified, all chemicals are from Aldrich and were used without further purification.

2.2. X-Band (9.5 GHz) ESR Measurements. X-band ESR spectra were recorded (in Prague) over the temperature range 110−280 K with a JEOL-PE-3X spectrometer equipped with an EC-100 computer interfaced to the PC Pentium 90 MHz. The dilute solutions of both copolymers were bubbled with nitrogen and filled into quartz capillaries. The measurements were performed with 100 kHz magnetic field modulation at a microwave output of 2 mW. The cavity temperature was stabilized with a JES-VT-3A temperature controller to ±0.5 K and measured with a platinum resistance thermometer. The magnetic field was measured with a MJ-110R NMR magnetometer (Radiopan Poznan). The *g*-factors were measured relative to the fourth line of the Mn^{2+} cation in the MgO ESR marker by taking $g = 1.981$ for this line.

2.3. Far-IR (250 GHz) ESR Measurements. The Cornell 250 GHz ESR spectrometer and its operation have been described elsewhere.[15,16] Dilute solutions of the spin-labeled copolymer in toluene were filled into reusable Teflon holders with flat windows which minimize interference with the millimeter-wave beam in the resonator. Because this holder is not sealable, the magnet bore was continuously purged with dry nitrogen gas to reduce line broadening from molecular oxygen. Such measures proved sufficient, since the residual oxygen broadening is generally much smaller than the ESR line widths in the slow-motional spectra at 250 GHz. The far-IR ESR spectra were recorded as a function of temperature in the range 110−372 K with a time constant of 1 or 3 s, a modulation amplitude ca. 5 G at 72.9 kHz, and a sweep field of about 500 G and then digitized to 1320 data points. The actual magnetic field values were calibrated using the far-IR ESR spectrum of a standard perdeuterated TEMPONE in toluene-d_8 sample at room temperature, whose splitting had been accurately measured earlier.[23] Before line-shape analysis, the phases of the experimental spectra were adjusted to correct for a slight admixture of the dispersion signal in a similar way to that described previously.[15]

2.4. Analysis of ESR Spectra. In the first step of the analysis, the **A** and **g** tensors of the spin-label attached to the polymer in toluene solution were obtained from the rigid limit spectra of the sample, which are only determined by the **A** and **g** tensors. Rigid limit spectra were calculated utilizing the EPRR program[9] and were fit to the experimental ones using a simple minimum least-squares fitting to obtain components of the **A** and **g** tensors. In suitable cases we have also used the slow-motional simulation program described below with rotational diffusion tensor components set at very low values. The principal axis systems of both tensors were considered identical, and their tensor components were assumed to be independent of the temperature.

Experimental slow-motional ESR spectra were calculated utilizing the spectral simulation method based on the stochastic Liouville equation.[9] The values of the **A** and **g** tensor components were fixed throughout all the simulations. The simulated spectra were fit to the experimental ones using a PC version of the nonlinear least-squares fitting program[24] NLSL based on a modified Levenberg−Marquart minimization algorithm[25,26] which iterates the simulations until a minimum least-squares fit to experiment is reached. This provides the optimum values for the fitted parameters, as well as estimates of error. The MOMD model for spin-label rotational diffusion was assumed. Input parameters include the parallel and perpendicular rotational diffusion coefficients $R_{\|}$ and $R_{\perp}$, the diffusion tilt β, the inhomogeneous [Lorentzian and/or Gaussian] line-width broadening, and the parameters c_0^2 and c_2^2 characterizing the orienting potential. When both c_0^2 and c_2^2 are zero, one then has simple Brownian rotational diffusion. All spectral simulations were performed on a 468 MHz PC equipped with two CELERON processors.

3. Results

3.1. Magnetic Tensors. An accurate determination of the components of the **A** and **g** tensors for the spin-label attached to a polymer chain in a particular solution is a necessary condition for obtaining reliable data characterizing its rotational diffusion. We have determined them in the usual way from rigid-limit ESR spectra of the copolymer measured in frozen toluene solution at 110 K at both frequencies as described above. The X-band rigid limit spectrum of the copolymer SL−ST−AA measured in frozen toluene solution at 110 K (Figure 1) was successfully fit using the NLSL program[24] and isotropic Brownian rotational diffusion of the spin-label using a very low value of $R = 1 \times 10^3$ s^{-1}. Best fits required axially symmetric Lorentzian inhomogeneous broadening characterized by the parameters $w_{\perp}$ and $w_{\|}$ and a Gaussian inhomogeneous broadening characterized by the width parameter gib0. This corresponds to a combined Lorentzian−Gaussian line shape frequently observed in rigid-limit spectra. It should be noted that the line shape of this well-resolved low-field spectrum (Figure 1) is very sensitive to the A_{xx}

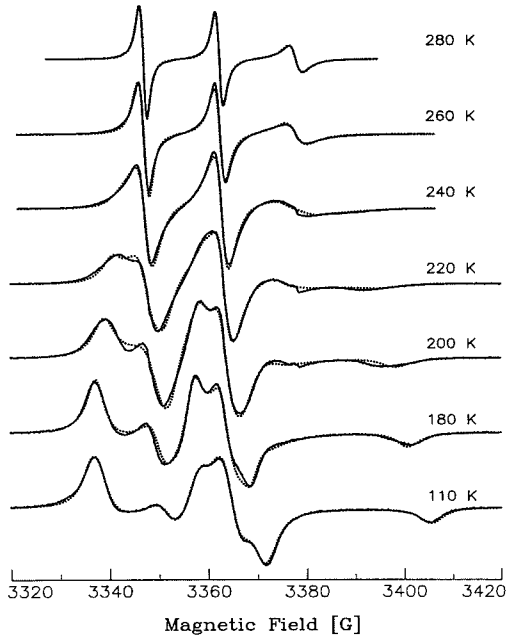

Figure 1. X-band ESR spectra of the copolymer SL−ST−AA in toluene at the given temperatures (experimental spectra, full lines; simulated spectra, dotted lines).

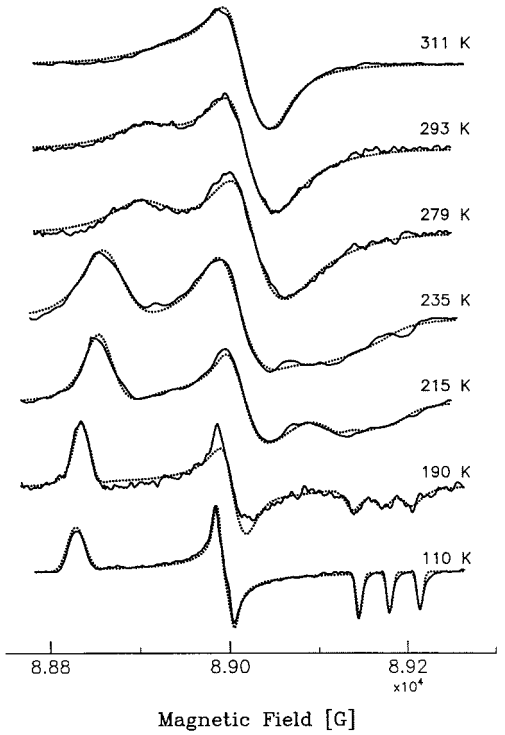

Figure 2. Far-IR ESR spectra of the copolymer SL−ST−AA in toluene at the given temperatures (experimental spectra, full lines; simulated spectra, dotted lines).

and A_{zz} values but less sensitive to the A_{yy} value. The uncertainty in A_{yy} was resolved by adopting the value calculated from the isotropic nitrogen hyperfine splitting (15.5 G) determined from the motionally narrowed three line low-field spectrum measured at 280 K (Figure 1).

Analysis of the far-IR ESR spectrum of the copolymer SL−ST−AA measured at 110 K (Figure 2) considered as a high-field rigid limit spectrum with the NLSL program would require an unrealistically large basis set. For this reason, we have used the rigid-limit EPRR program for the fitting, which proved very sensitive to the components of the **g** tensor but less sensitive to the **A** tensor components A_{xx} and A_{yy}. The spectrum was simulated assuming an orientation-dependent Lorentzian inhomogeneous broadening arising mainly from the expected g strain, so that it should be proportional to the absolute value of the respective **g**-tensor component (or more precisely its deviation from the free electron value). However, we found that such features also affected the A_{xx} and A_{yy} obtained without affecting the quality of the fit.

Finally, the line shapes of both the high- and low-field spectra of the SL−ST−AA copolymer in toluene at 110 K were successfully fit simultaneously to yield $g_{xx} = 2.010\ 00$, $g_{yy} = 2.006\ 27$, $g_{zz} = 2.002\ 10$, $A_{xx} = 6.11$ G, $A_{yy} = 6.09$ G, and $A_{zz} = 34.26$ G. The high-field spectrum yielded Lorentzian line widths: $w_{xx} = 10.9$ G, $w_{yy} = 5.09$ G, and $w_{zz} = 4.84$ G. The low-field spectrum yielded a combined Lorentzian−Gaussian line shape characterized by $w_{\perp} = 1.6$ G, $w_{\parallel} = 2.2$ G, and gib0 = 2.3 G.

3.2. X-Band ESR Spectra. ESR spectra of the SL−ST−AA copolymer in the temperature range studied are presented in Figure 1. Some of them (spectra measured at 200, 220, and 240 K) clearly indicate the presence of a small amount of much more mobile spin-label in the sample. We have frequently observed such a superposition in the ESR spectra of spin-labeled polymers in solutions, which is probably due to the slow detachment of some of the side chains through which the spin-label is connected to the main polymer chain, and it results in the appearance of a free nitroxide spectrum from the solution.

As a result of extensive calculations, we have found from both visual and statistical (e.g., the correlation coefficients obtained from the NLSL program) points of view that the best fits are obtained when using the MOMD model with axially symmetric Brownian rotational diffusion ($R_{\perp}$ and $R_{\parallel}$) and with a local potential as the model for spin-label reorientation. The MOMD model, when applied to the system of nitroxide spin-labels attached via short side chains (tethers) to the polystyrene main chain in solution, implies a preferred orientation for the axis of internal rotation of each attached nitroxide label with respect to the polymer main chain, but there is an isotropic distribution of these preferred orientations in the macroscopic sample due to the random distribution of polymer orientations. The nature of the preferred orientational distribution within each polymer is determined by the shape of the ordering potential, which may be varied by means of potential parameters c_0^2, c_2^2, c_0^4, etc., and optimized during the fitting process. The first two parameters were found to be sufficient in the present study.[24]

The optimum fits for all the low-field ESR spectra of the SL−ST−AA copolymer in toluene solution presented in Figure 1 were obtained for axially symmetric Brownian rotational diffusion of the nitroxide with the orientation of its symmetry axis relative to the principal axes of the nitroxide tensor of the rotational tensor characterized by the angle $\beta = 64 \pm 2°$ and by the ordering potential characterized by c_0^2 close to 0.6 and c_2^2 increasing with decreasing temperature from 0.3 to 1.1. The only exception to this was for the lowest temperature of 180 K, where somehwat larger values of c_0^2 and c_2^2 were found. Some spectra were slightly distorted by the presence of a small amount of the free nitroxide, but we did not use a two-site model for two reasons.

Table 1

T [K]	HF/LF	W_1	$R_\perp$ (10^8 s^{-1})	$R_\parallel$ (10^8 s^{-1})	c_0^2	c_2^2	β
311	HF	1.02	3.62	48.4	2.37	1.92	65.2
293	HF	0.12	2.37	25.1	2.40	1.86	64.1
280	LF	0.60	0.898	8.68	0.67	0.32	63.7
279	HF	0.01	1.93	18.4	2.08	1.78	65.3
260	LF	0.52	0.504	5.39	0.94	0.50	62.6
240	LF	0.09	0.088	5.11	0.66	1.02	64.0
235	HF	3.10	0.442	7.74	2.16	1.79	63.2
220	LF	0.10	0.0566	2.44	0.47	1.17	64.9
215	HF	2.50	0.151	4.27	2.35	1.90	63.6
200	LF	0.24	0.0349	0.78	0.57	1.14	64.2
190	HF	4.54	0.0053	0.35			65.0
180	LF	1.08	0.011	0.41	1.36	2.07	62.6

First, the parameters for the second site cannot be determined reliably due to its very low concentration (3−4% of the total spin-label). Second, the overall quality of the fit could not be increased in this way.

The values of the rotational tensor components and other parameters obtained are presented in Table 1 and in Figure 3.

3.3. Far-IR ESR Spectra. Good fits of the high-field ESR spectra of the toluene solutions of the copolymer SL−ST−AA in the temperature range studied (Figure 2) were also obtained using the MOMD model. However, there are systematic differences in the ordering potential parameters c_0^2 and c_2^2 and in the diffusion components $R_\perp$ and $R_\parallel$ when compared with the results obtained from the low-field spectra (cf. Table 1). The values of both c_0^2 and c_2^2 are systematically higher by factors of 2−5 compared to their low-field values. In addition, the high-field values of $R_\perp$ are about 2−4 times greater than their low-field values, while those of $R_\parallel$ are about 2 times larger than their low-field values above 200 K. The spectrum measured at 190 K is the only one that was not fit using the MOMD model, because its satisfactory fit would require an extremely large basis set, making it impractical to calculate. Thus, this spectrum was fit using a simple axially symmetric Brownian diffusion model.[24] All the values of the rotational tensor components and the other parameters are presented in Table 1 and in Figure 3.

3.4. Overall Fits. Arrhenius plots of $R_\perp$ and $R_\parallel$ were determined by fitting the results from both frequencies taken together and are presented in Figure 3. We are thereby neglecting the systematic differences between low- vs high-frequency results. Note that $R_\perp$ is at least an order of magnitude smaller than $R_\parallel$ at each temperature, with their difference becoming greater at the lower temperatures. The orientation of the rotational tensor symmetry axis in the *xz* plane of the nitroxide axis system characterized by the angle $\beta = 64 \pm 2°$ was determined by fitting both X-band and far-IR ESR spectra. This value agrees well with the orientation of the NH−C (Chart 1), which is expected to be the only bond contributing to the internal rotation of the spin-label with respect to the polymer chain segment, estimated from the crystal structure of the bis(2,2,6,6-tetramethyl-4-piperidinyl-1-oxy) suberate.[27]

4. Discussion

4.1. Segmental Diffusion. Several papers devoted to the study of segmental rotation in polymer chains using NMR and fluorescence techniques have been published in recent years. The correlation time, τ_c, for segmental rotational diffusion of polyisoprene in dilute solution was determined by ^{13}C NMR[4] and by measuring the depolarization of the fluorescence of the anthracene chromophore bound inside the polyisoprene main chain.[3] It was shown that Kramers's theory[28] in the high friction limit (eq 1 shown below with $\alpha = 1$) cannot accurately describe the segmental dynamics of this synthetic polymer in dilute solutions. For some polymers in solvents with high viscosity and large activation energy of the viscosity, E_η, the theory yields nonphysical negative values for the height of the potential barrier, E_a, for segmental rotation. That is, the prediction that the experimental correlation times should scale linearly with viscosity at constant temperature is generally not fulfilled. A power law relationship between τ_c and the solvent viscosity η was suggested[4] on the basis of papers published by Fleming and co-workers:[29]

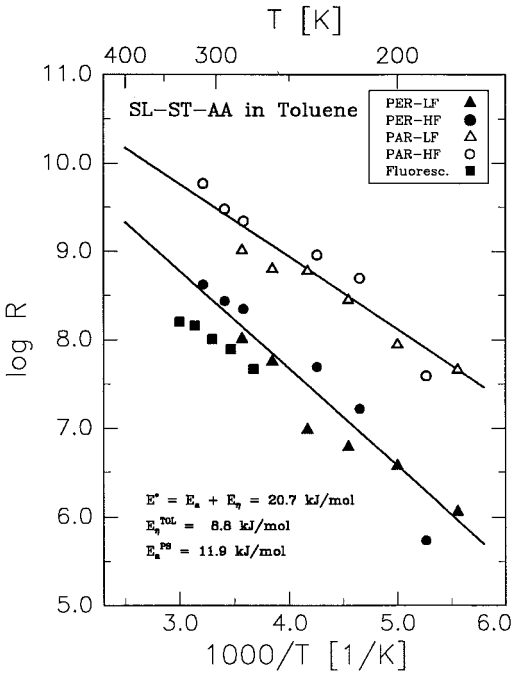

Figure 3. Arrhenius plots of the rotational diffusion coefficients $R_\perp$ and $R_\parallel$ for SL−ST−AA copolymer determined from the X-band (LF) and far-IR (HF) ESR spectra taken in dilute toluene solution. Values of the parameter $^1/_6\tau_c$ characterizing the rotational dynamics of anthracene chromophore located in the middle of polystyrene chain in 2-butanone solvent determined using fluorescence techniques taken from ref 2 are given for comparison (see text).

$$\tau_c = [\eta(\mathrm{T})]^\alpha \exp(E_a/RT) = \exp(E_{exp}/RT), \quad E_{exp} = E_a + \alpha E_\eta \quad (1)$$

with an exponent $0 \le \alpha \le 1$, where E_{exp} is the activation energy determined from an Arrhenius plot of τ_c or of R_S ($R_S = (6\tau_c)^{-1}$), similar to Figure 3. Also, E_a is the height of the potential barrier for segmental rotational motions, E_η is the activation energy for the viscous flow of the solvent, T is the absolute temperature, and R is the gas constant. The second equality of eq 1 is valid provided that the temperature dependence of the solvent viscosity exhibits Arrhenius behavior. The exponent α depends on the moment of inertia and size of the isomerizing unit and on the curvature at the top of the potential barrier. A larger size, or a larger moment of inertia, or a lower barrier will lengthen the time required to get across the barrier and thereby lead to a larger value of α. When this time is sufficiently length-

ened, then the high-frequency behavior of the friction is less significant, and behavior close to Kramers's high-friction limit should be observed. The value of the exponent α is expected to vary from polymer to polymer. The height of the intramolecular potential barrier E_a should not depend on the solvent in nonpolar systems.

For polyisoprene the values $E_a = 13 \pm 2$ kJ/mol and $\alpha = 0.41 \pm 0.02$ were found by ^{13}C NMR and the values $E_a = 10 \pm 1$ kJ/mol and $\alpha = 0.75 \pm 0.06$ by fluorescence depolarization. The difference in E_a is small and may be related to a modification of the potential barrier by the presence of the anthracene chromophore, because the fluorescence measurement senses the chain motion in the vicinity of anthracene. A larger size of the isomerizing unit and a larger moment of inertia due to the presence of the anthracene chromophore in the labeled chain would explain the higher α value determined by fluorescence depolarization.

Fluorescence depolarization has been used to determine the correlation time for the rotational diffusion of the anthracene chromophore bound inside a polystyrene main chain.[2] For polystyrene the value $\alpha = 0.90 \pm 0.05$, which was considered to be in reasonable agreement with Kramers's theory, was determined. The larger α observed for labeled polystyrene in comparison with labeled polyisoprene was rationalized by the presence of the bulky side groups of polystyrene. In this case, solvent-dependent heights of the potential barrier were observed to vary from $E_a = 8 \pm 2$ kJ/mol for a low-viscosity good solvent 2-butanone to $E_a = 21 \pm 2$ kJ/mol in cyclohexane. Also, a value of $E_a \cong 7$ kJ/mol was determined from the temperature dependence of the mean relaxation time of anthracene chromophore bound inside a polystyrene main chain in benzene solution by Horinaka et al.,[10] also using fluorescence depolarization.

Our ESR measurements of spin-labeled polystyrene presented in the Arrhenius plot for $R_\perp = R_S$ in Figure 3 yielded the value $E_{exp} = 20.7 \pm 1.5$ kJ/mol. The data for the low-viscosity good solvent 2-butanone determined by fluorescence[2] are presented in this figure for comparison. They are in surprisingly good agreement with ours, especially given that different labels and techniques were used. We used a value of $E_\eta = 8.8$ kJ/mol for the activation energy of viscous flow for toluene in the temperature range studied.[4] This is another good solvent for polystyrene. This yields a value of $E_a = 11.9 \pm 1.5$ kJ/mol for $\alpha = 1$. This value is in good agreement with the average value $E_a = 11$ kJ/mol found for the good solvents by fluorescence.[2] X-band measurements of the SL−ST−AA copolymer in several other solvents to study the effect of solvent quality and viscosity on the segmental dynamics of polystyrene are in progress.

4.2. Resolving the Discrepancy between High- and Low-Field Results. We now wish to discuss the systematic disparity between the high-field and low-field results for both the orientational potential coefficients and the rotational diffusion tensor coefficients, such that the high-field values were found to be systematically higher in both respects. These observations are very similar to those made by Barnes et al.[18] in a very recent 9 and 250 GHz study on the water-soluble protein T4 lysozyme. There they found that the potential coefficient c_0^2 measured at high field was about twice that measured at low field, and R (taken as isotropic) was about 4 times that at low field. They were able to resolve this discrepancy by introducing a more sophisticated model, known as the slowly relaxing local structure (SRLS) model.[19,30] A useful way of looking at this model in the present context is that it improves on the MOMD model by allowing for additional, slower motion of the rest of the large M_w polymer. That is, the MOMD model describes the polymer chain segmental motion as restricted by its attachments to the rest of the large M_w polymer; the SRLS model allows for additional slower motions. In the case of lysozyme, this slower motion was attributed to the overall tumbling of the protein. In fact, the analysis based on the SRLS model led to estimates of the overall tumbling rate that were in good agreement with previous determinations by other techniques.[18] The analysis of Barnes et al.[18] used the fact that at 250 GHz this overall motion was too slow to significantly affect the spectrum, so that the MOMD model was applicable. However, at 9 GHz this slower motion does affect the spectrum, and it therefore requires the SRLS model.[19] Consistency was found by using the 250 GHz results for the internal modes of motion and then imposing these values in the SRLS model to yield the overall motional rate from the 9 GHz spectra.

The trends of slower diffusion and smaller potential from the 9 GHz spectrum when only the MOMD model was used could be simply rationalized as follows.[18] The effective motion (from the MOMD perspective) at 9 GHz is a combination of both the faster internal and the slower overall motions; hence, it should be described by an intermediate motional rate that is slower than that for internal motions. Also, since the overall motion is unconstrained, the effective potential of the combined constrained internal and free overall motions should be reduced from just that for the internal motion. This appears to also be appropriate for the results of the present study. [In other work, the SRLS model has been employed in CW-ESR studies of rotational dynamics in DNA oligomers[31] and in a two-dimensional ESR study on a polymer liquid crystal.[32]]

It thus seems reasonable to suppose that the use of the SRLS model with its more sophisticated (and challenging) analysis would resolve the present discrepancy between the MOMD-analyzed 9 and 250 GHz results on this spin-labeled polystyrene polymer. The question remains whether the additional (slower) motion be attributed to the overall tumbling or to slower polymer segmental motions. The hydrodynamic radius R_H of 9 nm measured for this polymer (cf. section 2.1) in toluene yields an $R_{overall} \sim 10^7$ s^{-1} at 300 K and about 5 times smaller at 250 K. Indeed, these are values that should affect the 9 GHz spectra but not the 250 GHz spectra, as discussed above.[18,31] Such values of $R_{overall}$ are in fact of the magnitude that can yield the discrepancies between the $R_\perp$ values from 9 GHz vs 250 GHz in Table 1 and Figure 3.

These observations support our belief that a multi-frequency ESR study should enable one to decompose the different modes of the complex dynamics of a polymer in dilute solution on the basis of the different time scales associated with ESR spectra taken at different frequencies.

5. Conclusions

A styrene copolymer containing less than 5 mol % of spin-labeled chain units distributed randomly along the polymer main chain was synthesized. The parameters R_S and R_I characterizing rotational diffusion of the spin-label attached to the polystyrene main chain via a short tether have been determined by means of fitting ex-

perimental ESR spectra of the copolymer measured at X-band (9 GHz) and at far-IR (250 GHz) in dilute toluene solution over a broad temperature range to the MOMD model. Both the parameter R_S for the segmental rotational diffusion in the polystyrene chain and the height of the potential barrier for conformational transitions in the polystyrene chain, $E_a = 11.9 \pm 1.5$ kJ/mol, were found to be in good agreement with published results obtained for dilute polystyrene solutions in good solvents by fluorescence depolarization. The different results for the ordering potential parameters and the rotational diffusion rates from X-band vs FIR, which were found by least-squares fits to the experimental spectra using the MOMD model for the dynamics of spin-labels in the solution, have been interpreted in terms of the lower sensitivity of the far-IR (but not the X-band) ESR spectra to slower motions, such as the overall polymer tumbling.

Acknowledgment. Members of the Czech part of the team (J.P., J.L., and A.M.) wish to acknowledge support from the Grant Agency of the Academy of Sciences of the Czech Republic (grant A4050804) and from a grant of the Ministry of Education of the Czech Republic (grant KONTAKT ME 149). We thank Dr. Petr Štepánek (IMC Prague) for his assistance with the DLS experiments. The U.S. team acknowledges the support of the NSF and the NIH.

References and Notes

(1) Ediger, M. D. *Annu. Rev. Phys. Chem.* **1991**, *42*, 225.
(2) Waldow, D. A.; Ediger, M. D.; Yamaguchi, Y.; Matsushita, Y.; Noda, I. *Macromolecules* **1991**, *24*, 3147.
(3) Adolf, D. B.; Ediger, M. D.; Kitano, T.; Ito, K. *Macromolecules* **1992**, *25*, 867.
(4) Glowinkowski, S.; Gisser, D. J.; Ediger, M. D. *Macromolecules* **1990**, *23*, 3520.
(5) Spyros, A.; Dais, P.; Heatley, F. *Macromolecules* **1994**, *27*, 6207.
(6) Pilar, J.; Labský, J. *J. Phys. Chem.* **1986**, *90*, 6038.
(7) Pilar, J.; Labský, J. *Macromolecules* **1991**, *24*, 4188.
(8) Pilar, J.; Labský, J. *Macromolecules* **1994**, *27*, 3977.
(9) Schneider, D. J.; Freed, J. H. In *Biological Magnetic Resonance*; Berliner, L. J., Reuben, J., Eds.; Plenum: New York, 1989; Vol. 8, p 1.
(10) Horinaka, J.; Aoki, H.; Ito, S.; Yamamoto, M. *Polym. J.* **1999**, *31*, 179.
(11) Horinaka, J.; Ito, S.; Yamamoto, M.; Tsujii, Y.; Matsuba, T. *Macromolecules* **1999**, *32*, 2270.
(12) Bahar, I.; Erman, B.; Monnerie, L. *Macromolecules* **1990**, *23*, 1974.
(13) Mason, R. P.; Polnaszek, C. F.; Freed, J. H. *J. Phys. Chem.* **1974**, *78*, 1324.
(14) Meirovitch, E.; Nayeem, A.; Freed, J. H. *J. Phys. Chem.* **1984**, *88*, 3454.
(15) Budil, D. E.; Earle, K. A.; Freed, J. H. *J. Phys. Chem.* **1993**, *97*, 1294.
(16) Earle, K. A.; Budil, D. E.; Freed, J. H. *J. Phys. Chem.* **1993**, *97*, 13289.
(17) Earle, K. A.; Moscicki, J.; Polimeno, A.; Freed, J. H. *J. Chem. Phys.* **1997**, *106*, 9996.
(18) Barnes, J.; Liang, Z.; Mchaourab, H.; Freed, J. H.; Hubbell, W. *Biophys. J.* **1999**, *76*, 3298.
(19) Liang, Z.; Freed, J. H. *J. Phys. Chem. B* **1999**, *103*, 6384.
(20) Labský, J.; Pilar, J.; Lövy, J. *J. Magn. Reson.* **1980**, *37*, 515.
(21) Jakeš, J. *Collect. Czech. Chem. Commun.* **1995**, *60*, 1781.
(22) Štepánek, P. In *Dynamic Light Scattering: The Method and Some Applications*; Brown, W., Ed.; Oxford University Press: New York, 1993.
(23) Hwang, J. S.; Mason, R. P.; Hwang, L.-P.; Freed, J. H. *J. Phys. Chem.* **1975**, *79*, 489.
(24) (a) Budil, D. E.; Lee, S.; Saxena, S.; Freed, J. H. *J. Magn. Reson.* **1996**, *A120*, 155. (b) The calculation for $R = 1 \times 10^3$ s^{-1} (i.e., the rigid limit) at 9 GHz converged very well when using a quite tractable basis set characterized by the parameters lemx = 40, lomx = 39, kmx = 16, mmx = 2, and ipnmx = 2. For the 9 GHz motional spectra a tractable basis set characterized by the parameters lemx = 14, lomx = 11, kmx = 8, mmx = 8, and ipnmx = 2 was found sufficient and was used for nearly all calculations. For the 250 GHz spectrum at 190 K a basis set characterized by the parameters lemx = 50, lomx = 41, kmx = 16, mmx = 16, and ipnmx = 2 was required.
(25) Dennis, J. E., Jr.; Schnabel, R. B. *Numerical Methods for Unconstrained Optimalization and Nonlinear Equations;* Prentice Hall: Englewood Cliffs, NJ, 1983.
(26) More, J. J.; Garbow, B. S.; Hilstron, K. E. *User's Guide for MINPACK-1;* National Technical Information Service: Sprinfield, VA, 1980.
(27) Capiomont, A. *Acta Crystallogr., Sect. B* **1972**, *28*, 2298.
(28) Kramers, H. A. *Physica* **1940**, *7*, 284.
(29) Courtney, S. H.; Fleming, G. R. *J. Chem. Phys.* **1985**, *83*, 215.
(30) Polimeno, A.; Freed, J. H. *J. Phys. Chem.* **1995**, *99*, 10995.
(31) Liang, Z.; Freed, J. H.; Keyes, R. S.; Bobst, A. M. *J. Phys. Chem.*, in press.
(32) Xu, D.; Crepeau, R. H.; Ober, C. K.; Freed, J. H. *J. Phys. Chem.* **1996**, *100*, 15873.

MA0002242